Enhancement of crossed Andreev reflection in a superconducting ladder connected to normal metal leads

Abhiram Soori[1] and Subroto Mukerjee[2]
[1]*International Centre for Theoretical Sciences, Tata Institute of Fundamental Research, Survey No. 151, Shivakote, Hesaraghatta Hobli, Bengaluru North 560089, India*
[2]*Department of Physics, Indian Institute of Science, Bengaluru 560012, India*
(Received 2 May 2016; revised manuscript received 24 February 2017; published 23 March 2017)

Crossed Andreev reflection (cAR) is a scattering process that happens in a quantum transport setup consisting of two normal metals (NM) attached to a superconductor (SC), where an electron incident from one NM results in a hole emerging in the other. Typically, electron tunneling (ET) through the superconductor from one NM to the other competes with cAR and masks its signature in the conductance spectrum. We propose a scheme to enhance cAR, in which the SC part of the NM-SC-NM is side coupled to another SC having a different superconducting phase to form a Josephson junction in the transverse direction. At strong enough coupling and for a large enough phase difference, one can smoothly traverse between the highly ET-dominant to the highly cAR-dominant transport regimes by tuning chemical potential, due to the appearance of subgap Andreev states that are extended in the longitudinal direction. We discuss connections to realistic systems.

DOI: 10.1103/PhysRevB.95.104517

I. INTRODUCTION

Andreev reflection (AR) is the scattering process by which a current flows across the interface of a normal metal (NM) and a superconductor (SC) when an external bias across the interface is applied in the subgap regime. The Cooper-pair current in the superconductor draws equal contributions from the electron and hole channels of the normal metal. This phenomenon, first discovered by Andreev [1], has been extensively studied theoretically and experimentally for several decades [2–4].

AR has played an important role in the observation of transport signatures of exotic Majorana fermions in mesoscopic systems [4]. In addition, recent advances in cold-atomic systems promise new testbeds where theoretical findings [5,6] related to Andreev reflection can be demonstrated experimentally [7]. Crossed Andreev reflection (cAR) is a phenomenon closely related to AR and occurs in a system consisting of two normal metals attached to a superconductor [8–21]. An electron incident on the SC from the first normal metal (NM1) gets absorbed into the SC as a Cooper pair, absorbing the second electron of the Cooper pair from the second normal metal (NM2), resulting in a hole current in NM2. The phenomenon of cAR is closely related to the production of nonlocally entangled electrons by splitting Cooper pairs from the SC, the detection and enhancement of which has seen a lot of theoretical [22] and experimental interest [23,24]. However, cAR is accompanied by electron tunneling (ET) where the electron from NM1 tunnels into NM2 as an electron. cAR is typically masked in simple NM-SC-NM systems due to dominant ET [9]. A negative differential transconductance between NM1 and NM2 is a definite signature of cAR.

In this paper, we propose a scheme to enhance cAR, which is different from other existing proposals [10–18], and demonstrate with a simple theoretical model that cAR enhancement can be much greater than predicted in them. Of the two existing proposals that have been experimentally realized, the first method introduces barriers at the NM-SC junctions of an NM-SC-NM setup [16,20], while the second employs two ferromagnets (FM) in an antiparallel configuration instead of the NM's [17–19] that suppress ET and AR thereby allowing cAR to dominate. cAR is enhanced in the former method when the momentum scale characterizing the barrier is at least as large as the Fermi momentum, though the enhanced cAR currents are too small as shown in Appendix A. In addition, there are several other proposals such as: (i) employing quantum spin Hall insulators connected to SC and spatially separate ET and cAR channels based on the spin-momentum locking of the edge states [11], (ii) driving a steady Cooper pair current in the SC such that the SC phase modulates and thus enhances cAR [12], (iii) substituting NM and SC parts of the setup with exotic materials such as graphene, silicene, topological insulators, and topological superconductors [13,14], (iv) coupling to external electromagnetic modes [15], which have not yet been realized experimentally.

Here, we propose to modify the NM-SC-NM setup by side coupling the SC with another SC (which has a superconducting phase differing by ϕ but the same magnitude of the pair potential) as shown in Fig. 1(a). We call the two coupled SC's together an 'SC ladder' (note that this is different from several setups such as the one by Grosselin *et al.* [25] where a magnetic flux enclosed between two superconductors forming a loop can control subgap transport in the superconductors). We show that an adequate superconducting phase difference between two legs of the ladder accompanied by a sufficiently strong coupling between two legs of the SC ladder leads to subgap Andreev states which can enhance cAR. This is the central result of our work.

II. DETAILS OF THE CALCULATION

A. Hamiltonian and dispersion

Introducing the hole annihilation operators $d_{s,\lambda}(x)=c^{\dagger}_{\bar{s},\lambda}(x)$, the Hamiltonian for the ladder region ($0 \leqslant x \leqslant a$) can be

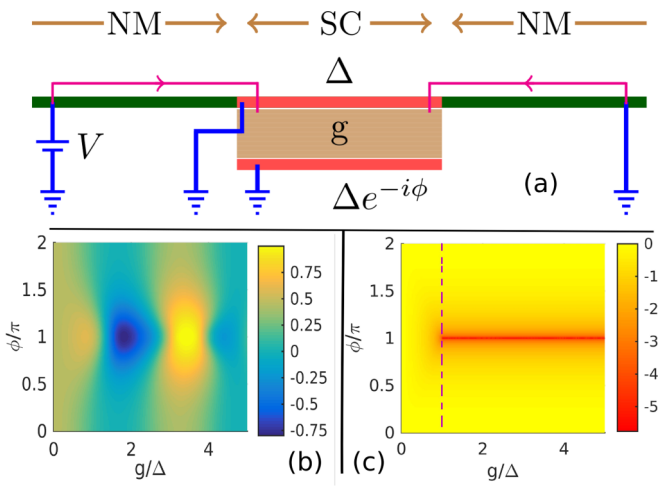

FIG. 1. (a) A schematic diagram of the setup. The thick red lines in the middle are the two SC channels, coupled to each other by a strength g highlighted by the brown region in between. A voltage bias V is applied to the left NM while the SC ladder and the right NM are grounded, as shown by the blue lines. Thin lines with arrows show the current directions when cAR dominates over ET. (b) The zero bias transconductance G_{RL} in units of $2e^2/h$. (c) The logarithm of the gap in the dispersion of the ladder region [Eq. (2)] in units of Δ; the vertical dashed line corresponds to $g/\Delta = 1$. The parameters chosen are $\mu = 10\Delta$, $a = 6\hbar/\sqrt{2m\Delta}$.

written as:

$$H = \sum_{\lambda,s}\Big[\Psi^{\dagger}_{s,\lambda}(x)\Big\{\Big(\frac{-\hbar^2}{2m}\frac{\partial^2}{\partial x^2} - \mu\Big)\tau_z + \Delta(\cos\phi_\lambda\tau_x + \sin\phi_\lambda\tau_y)\Big\}\Psi_{s,\lambda}(x) + g\Psi^{\dagger}_{s,\lambda}(x)\tau_z\Psi_{s,\bar{\lambda}}(x)\Big], \quad (1)$$

where (i) $s = \uparrow, \downarrow$ and $\lambda = 1,2$ are spin and wire indices, respectively, (ii) $\bar{s}/\bar{\lambda}$ takes the value of the label index different from s/λ, and (iii) $\Psi_{s,\lambda}(x) = [\sigma_s c_{s,\lambda}(x), d_{s,\lambda}(x)]^T$, where $\sigma_{\uparrow/\downarrow} = \pm 1$. The dispersion for this Hamiltonian is:

$$E = \pm\sqrt{\epsilon_k^2 + g^2 + \Delta^2 \pm 2g\sqrt{\epsilon_k^2 + \Delta^2\sin^2[(\phi_1 - \phi_2)/2]}}, \quad (2)$$

where $\epsilon_k = (\hbar^2k^2/2m - \mu)$ and $\hbar k$ is the momentum. Each of these bands is doubly degenerate due to spin ($s = \uparrow, \downarrow$). The Hamiltonians for the NM regions on the left ($x < 0$) and right ($x > a$) are $H = \sum_s c_s^{\dagger}(x)[\hbar^2k^2/2m - \mu]c_s(x)$. From here onwards, we shall leave out the spin index s and a factor of 2 to account for spin degeneracy will multiply the conductances in the final result. The superconducting phases ϕ_λ on the two legs ($\lambda = 1,2$) of the SC ladder can be chosen to be $\phi_1 = 0$, and $\phi_2 = -\phi$, without loss of generality so that $(\phi_1 - \phi_2) = \phi$.

B. Wave function

The solution to the Hamiltonian is a two-spinor ψ in the NM regions (the two components represent the electron and hole channels) and a four-spinor $[\psi^T, \chi^T]^T$ in the ladder region (two more components represent the second leg of the ladder), where the spinors ψ and χ have the form: $\psi(x) = [\psi_e(x), \psi_h(x)]^T$ for $-\infty < x < \infty$ and $\chi(x) = [\chi_e(x), \chi_h(x)]^T$ for $0 \leqslant x \leqslant a$. In the NM regions, the electrons and holes have momenta $\pm\hbar k_e$ and $\pm\hbar k_h$, respectively, where $k_{e/h} = \sqrt{2m(\mu \pm E)/\hbar^2}$ at a given energy E. The scattering wave function for an electron incident from the left onto the ladder region at an energy E is given by:

$$\begin{aligned}
\psi_e(x) &= e^{ik_e x} + r_n e^{-ik_e x}, \quad \text{for } x \leqslant 0,\\
&= t_n e^{ik_e x}, \quad \text{for } x \geqslant a,\\
\psi_h(x) &= r_a e^{ik_h x}, \quad \text{for } x \leqslant 0,\\
&= t_a e^{-ik_h x}, \quad \text{for } x \geqslant a,\\
\psi(x) &= \sum_{\sigma,\nu,p} s_{\sigma,\nu,p} e^{i\sigma k_{\nu,p} x}[\psi_{e,\nu,p}, \psi_{h,\nu,p}]^T \quad \text{and}\\
\chi(x) &= \sum_{\sigma,\nu,p} s_{\sigma,\nu,p} e^{i\sigma k_{\nu,p} x}[\chi_{e,\nu,p}, \chi_{h,\nu,p}]^T,\\
&\quad \text{for } 0 \leqslant x \leqslant a. \qquad (3)
\end{aligned}$$

In the ladder region, the momenta $\sigma\hbar k_{\nu,p}$ at energy E denoted by the indices σ, ν, p are obtained by inverting the dispersion relation Eq. (2): $\hbar k_{\nu,p} = \sqrt{2m(\sigma_p\epsilon_{k,\nu} + \mu)}$, where $\epsilon_{k,\nu} = \sqrt{E^2 + g^2 - \Delta^2 + 2g\nu\sqrt{E^2 - \Delta^2\cos^2(\phi/2)}}$, and the index $\sigma = \pm 1$ denotes whether the mode is for a right/left mover, the index $\nu = \pm 1$ refers to the antibonding/bonding bands formed due to the hybridization between the two legs ($\lambda = 1,2$) of the ladder, and $p = e,h$ refers to electron, holelike bands for which $\sigma_{e/h} = \pm 1$.

C. Boundary conditions

From the boundary conditions (BC's) described by Carreau *et al.* [26] for a general one-dimensional system, we choose the one that is physically relevant to our system. The NM-SC junction generically has a barrier for electron tunneling which limits the electron transmission. The BC at the NM-SC interface is described by the continuity of the wave function and a discontinuity of the derivative [2]. The latter is the same as having a delta-function barrier potential on the NM side of the NM-SC junction, infinitesimally close to the junction. Since we are interested in enhancing cAR over ET, we set the barrier strengths to zero to make the NM-SC junctions fully transparent. In other words, both the wave function and its derivative at the NM-SC interface are continuous. But this fixes the BC only for one leg of the ladder. The BC for the other leg is given by a probability current conserving BC at the ends of the ladder (i.e., $x = 0,a$). Such a BC that describes the lower leg of the ladder depends on four parameters in general as for the 'particle in a box' study of Carreau *et al.* [26]. The NM-SC interfaces at $x = 0,a$ are not connected by any direct hopping as in the case of periodic BC's. This causes the BC's to depend on just two parameters: $(q_{2,x_0} + \partial_x)\Psi_2(x)|_{x=x_0} = 0$, where q_{2,x_0} is a real-valued parameter with dimensions of inverse length that describes the BC at x_0. The limit $q_{x0} \to \infty$ implies that the wave function is zero at $x = x_0$, while the limit $q_{x0} \to 0$ implies that the first derivative of the wave function is zero at x_0, allowing the wave function to have a nonzero probability density at x_0. The latter limit qualitatively

corresponds to a lattice model of the SC ladder in which the last site of the second leg can have a finite probability density. Hence, we have chosen $q_{x_0} = 0$ for both $x_0 = 0$ and $x_0 = a$, though a particular choice of the BC does not affect the results qualitatively. The BC's used are:

$$\psi(x_0^+) = \psi(x_0^-), \partial_x\psi(x)|_{x=x_0^+} = \partial_x\psi(x)|_{x=x_0^-},$$
$$\partial_x\chi(x)|_{x=x_0} = 0 \quad \text{for } x_0 = 0, a. \tag{4}$$

Both the NMs are connected to only one leg ($\lambda = 1$) of the SC ladder as shown in Fig. 1(a). As mentioned earlier, the junction is modeled to be transparent since we are interested in enhancing cAR, a scattering process which involves both the NMs. We first calculate the scattering amplitudes numerically for a diverse set of relevant parameters by employing the BC: Eq. (4) in the wave function given by Eq. (3). Using these scattering amplitudes, the transconductance is calculated, which is the physical quantity of interest since it can be experimentally measured.

D. Transconductance

The system under investigation is essentially a three terminal setup. The NM regions on the left and right (extending to $x \to \mp\infty$) form two terminals and the SC ladder in the middle (maintained at a fixed chemical potential μ) acts as a reservoir for the charge current since it is not conserved in the SC region.

We are interested in calculating the differential transconductance $G_{RL}(V) := dI_R(V)/dV$, where $dI_R(V)$ is the change in current in the right NM when the Fermi energy of the left NM is changed from eV to $e(V + dV)$, keeping the Fermi energies of the ladder region and right NM at zero (here, e is the electronic charge and V is the voltage). Using the Landauer-Büttiker formalism [27], the differential transconductance in such a transport setup at a bias voltage V is

$$G_{RL}(V) = \frac{2e^2}{h}(|t_n|^2 - |t_a|^2\sqrt{(\mu - eV)/(\mu + eV)}). \tag{5}$$

It is easy to see from Eq. (5) that the contributions of ET and cAR to the current on the right NM are positive and negative, respectively. Hence, a negative G_{RL} is a clear signature of cAR enhanced over ET while a positive G_{RL} implies the dominance of ET over cAR.

III. RESULTS

(1) The zero-bias transconductance $G_{RL}|_{V=0}$ as a function of the parameters ϕ and g is shown in Fig. 1(b) and we understand it in terms of the dispersion of the ladder region given by Eq. (2). Figure 1(c) is a contour plot of the logarithm of the gap in units of Δ (i.e., $\log[E_g/\Delta]$). The gap closes on the line: $g/\Delta \geqslant 1, \phi = \pi$. cAR is enhanced as g/Δ crosses 1 from left to right, and this enhancement is prominent around $0.7\pi < \phi < 1.3\pi$ and $1.4\Delta < g < 2.2\Delta$. Further, as g/Δ crosses a value of 3, ET is enhanced to a value as high as $\sim 0.75 \times 2e^2/h$. This indicates that the enhancement of cAR and ET to such high values is related to the closing of the gap.

(2) Fixing $\phi = \pi$, we see how the subgap conductance spectrum changes as the coupling strength g is changed.

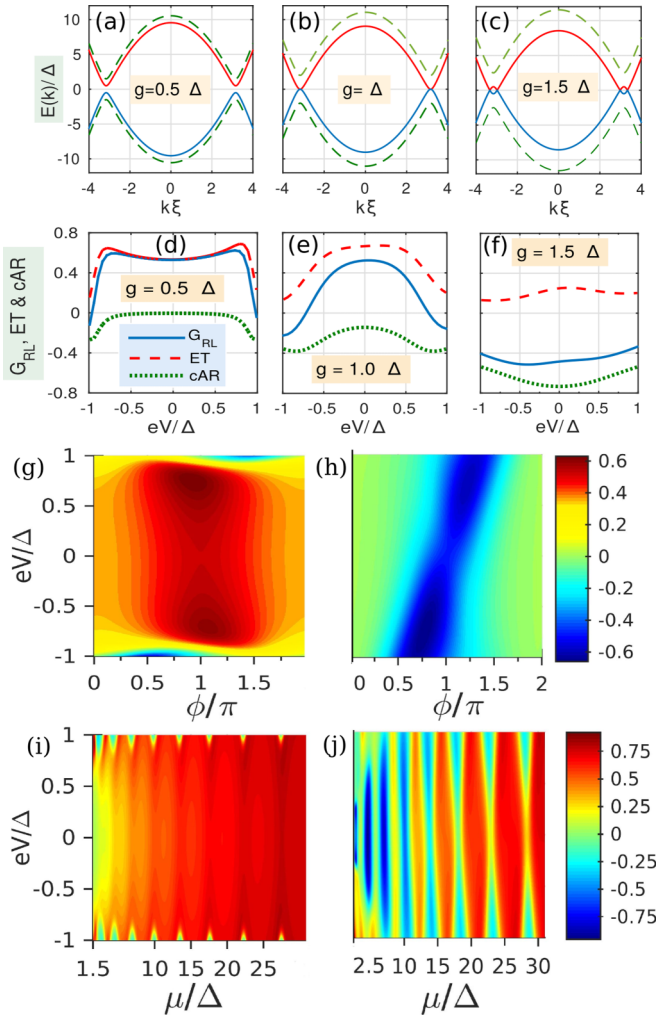

FIG. 2. (a)–(c): Dispersion of the SC ladder, (d)–(f): transconductance G_{RL}, contributions to it from ET and cAR for $\phi = \pi, \mu = 10\Delta$. (g)–(j): Contour plots of G_{RL}. For (g),(i), $g = 0.5\Delta$. For (h),(j), $g = 1.5\Delta$. For (d)–(j), $a = 6\hbar/\sqrt{2m\Delta}$. For (g),(h), $\mu = 10\Delta$. For (i),(j), $\phi = \pi$. G_{RL} is in units of $2e^2/h$.

This is contrasted with the dispersion of the ladder region, the topology of which changes when g/Δ is on either side of 1. In Figs. 2(a)–2(c), the dispersion of the SC ladder, and in Figs. 2(d)–2(f), the conductance spectrums for $g/\Delta = 0.5, 1.0, 1.5$ have been plotted. As g/Δ crosses over from 0.5 to 1.5, through 1.0, the conductance spectrum shifts smoothly from being in the positive half to being in the negative half of the ordinate, which is a clear signature of enhanced cAR as indicated by the green dotted lines. This enhancement is accompanied by the appearance of subgap Andreev states in the SC ladder.

(3) The dependence of the conductance spectrum in the bias window ($|eV| \leqslant \Delta$) on the superconducting phase difference ϕ and the chemical potential μ can be obtained. Figures 2(g)–2(h) shows contour plots of G_{RL} as a function of (eV, ϕ) for $g = 0.5\Delta$ [2(g)] and $g = 1.5\Delta$ [2(h)]. One can see that cAR is enhanced significantly for the case $g = 1.5\Delta$ throughout in the bias window $(-\Delta, \Delta)$, and the value of ϕ at which cAR is enhanced the most depends on the value of the

bias eV. Though cAR is enhanced in the case of $g = 0.5\Delta$, this happens in very narrow regions of the eV-ϕ plane, and it is worth noting that the enhancement of cAR for $g = 0.5\Delta$ happens for values of ϕ far away from zero or 2π.

(4) Figures 2(i)–2(j) show contour plots of G_{RL} as a function of (eV,μ) for $g = 0.5\Delta$ [2(i)] and $g = 1.5\Delta$ [2(j)]. For these two cases, $\phi = \pi$. It is apparent from the contour plots that the enhancement of cAR is prominent in the case of $g = 1.5\Delta$ compared to the case of $g = 0.5\Delta$. For $g = 1.5\Delta$, cAR is enhanced throughout the bias window around certain values of μ, but for $g = 0.5\Delta$, a poor cAR enhancement can be found in very small regions near $eV = \pm\Delta$. Further, the enhancement of cAR occurs at a series of μ_i's. Also, the enhancement of cAR around the μ_i's becomes less prominent with increasing μ_i.

IV. MECHANISM

The above results point to the following mechanism for the enhancement of cAR: A nonzero phase difference ϕ and a nonzero coupling g between the two legs of the ladder create plane-wave modes within the otherwise gapped dispersion of the ladder region as can be seen from Eq. (2). Equivalently, two out of four $k_{v,p}$'s become real valued at energies: $|E| < \Delta$. These plane wave modes have nonzero components in both electron and hole sectors, and we call them subgap Andreev states. Thus, the transconductance is due to a Fabry-Pérot type interference between the subgap Andreev states in the ladder region that transmit either an electron or a hole into the right NM. The probabilities of the two transmission processes can be tuned by changing a parameter that changes the dispersion and the spinor structure of the modes in the ladder region. The subgap Andreev states can be thought of as plane wave modes formed by the hybridization of Andreev bound states, when a large number of Josephson junctions (each formed between two superconducting quantum dots) are coupled.

Since, the chemical potential μ sets the fundamental length scale of the problem and affects the spinor structure of the BdG modes, changing μ smoothly, keeping the values of eV, ϕ ($\neq 0$) and g ($\neq 0$) fixed must show a smooth transition from maximally enhanced cAR to maximally enhanced ET. This can be seen in Fig. 2(j), and the recurrent enhancement of cAR and ET at a series of values of μ ($= \mu_i$) corresponds to a periodicity in k_i's (where $k_i = \sqrt{2m\mu_i/\hbar^2}$) [28], given by $(k_{i+1} - k_i)a \sim \pi$, reaffirming quantitatively our explanation that the cAR enhancement is due to Fabry-Pérot interference between the subgap Andreev states in the SC ladder. As can be seen from Fig. 1(c), $\phi = \pi$ and $g > \Delta$ give rise to gap closing and hence the cAR enhancement is expected to be maximal for this choice of parameters, which is in agreement with the results highlighted in Figs. 2(d)–2(j).

V. DISCUSSION

We have primarily studied a one-dimensional superconductor side coupled to another one-dimensional superconductor having a superconducting phase different from the first superconductor. However, long-range superconducting order is not possible in purely one dimension. This limitation can be overcome by a proximate higher dimensional superconductor in contact with the one-dimensional quantum wire. Also, the Fermi energy and chemical potential in the SC are assumed to be maintained at particular values, which means that a steady state current flows into the SC and the SC is grounded via a grounding electrode.

We now discuss different systems that are closer to experimental setups in which our results can possibly be tested. To be able to maintain a SC phase difference ϕ between two legs of the ladder is an important task when it comes to experimental implementation. We make the following proposals to achieve this [29]:

(1) Passing a supercurrent in the transverse direction; a SC phase difference between two legs of the SC ladder is induced that is proportional to the transverse current [12].

(2) Using magnetic flux to mimic the Josephson phase difference as in SQUIDS [30]. Connecting two legs of the ladder through a loop and passing a magnetic flux through can induce a phase difference proportional to the flux (modulo flux quantum Φ_0) as discussed in Ref. [31].

(3) Using π-junction materials, such as layered superconductors [32] which have a nonzero superconducting phase difference naturally existing between the adjacent layers is one direction. Sandwiching such a layered SC between NM leads in such a way that each layer lies in the longitudinal direction can mimic the ladder structure proposed here. This will be a quasi-two-dimensional version of the setup we have proposed. We have performed transport calculations for such a two-dimensional version of the ladder geometry and we see that most of our results we obtained above remain the same qualitatively.

(4) In a closely related system namely *a Josephson junction between two-dimensional superconductors*, subgap Andreev states appear. To describe the system more precisely, let the regions $(0 \leqslant y \leqslant \infty, 0 < x < a)$ and $(-\infty < y < 0, 0 < x < a)$ have SC phases Δ and $\Delta e^{-i\phi}$. Using appropriate BC at $y = 0$, the subgap states localized at the junction can be calculated (see Appendix B). We see that very similar to the ladder, a nonzero ϕ gives rise to subgap states which are BdG plane-wave modes along the x direction, but are localized in the y direction around $y = 0$. These states can be used to enhance cAR if two NM metal leads are connected close to the Josephson junction.

The very fact that a phase difference is maintained between the two legs of the ladder means that a Josephson current flows from one leg of the ladder to the other in the transverse direction. However, this current does not interfere with the quasiparticle current that is carried by the subgap Andreev states between the two NM leads. In a recent experiment [33], it was demonstrated that a subgap Andreev bound state formed in a Josephson junction shows a subgap peak in conductance when connected to a NM. This is due to Andreev reflection, and the current in the NM due to Andreev reflection does not interfere with the Josephson current that flows from one SC to the other. The existence of stabilized subgap modes is required to obtain enhanced cAR.

In a setup where cAR is enhanced over ET and AR, if the bias is maintained across both the NM-SC junctions keeping the two NM's grounded, a high-efficiency Cooper pair splitting (CPS) results. Once a considerable superconducting phase difference ($\pi/2 \lesssim \phi \lesssim 3\pi/2$) is maintained in the ladder, CPS

can be enhanced by tuning either the chemical potential μ or the length a of the ladder region, in contrast to the already existing Cooper pair splitter [23,24] which is based on Coulomb blockaded quantum dots, where two gate voltages need to be tuned to a particular combination. In this respect, our scheme may be more robust to the parameters that need to be tuned to get CPS enhancement. Further, the conductances measured in the experiment reporting high efficiency CPS [24] suggest that the corresponding cAR enhanced transconductance values are much smaller in magnitude than the values that can be obtained theoretically in our setup.

ACKNOWLEDGMENTS

A.S. thanks Diptiman Sen, G Baskaran, Anindya Das, Oindrila Deb, Aviad Frydman, Efrat Shimshoni, Pascal Simon, Ady Stern, Manisha Thakurati, Aveek Bid, Hemanta Kundu, and Alfredo Levy Yeyati for discussions. A.S. thanks Abhishek Dhar for support and encouragement and *Infosys Excellence Grant for* ICTS-TIFR, *Bengaluru* for funding expenses to participate in *APS March meeting 2016*, where this work was presented. We thank Diptiman Sen for careful reading of the manuscript.

APPENDIX A: NM-SC-NM WITH BARRIERS

Chtchelkatchev [16] has performed calculations for a two-dimensional NM-SC-NM system with barriers at the junctions. We study the one-dimensional version of the NM-SC-NM setup with barriers here and reproduce their results qualitatively, i.e., show that cAR is enhanced by having barriers at the NM-SC interface. Figure 3 summarizes the results of our calculations on a single-channel SC connected to two NM leads with barriers of strength $q_0 = 5k_F$ (where $k_F = \sqrt{2m\mu/\hbar^2}$). The parameter q_0 enters the calculations through the BC:

$$\partial_x \psi(x)|_{x=\pm a+0} - \partial_x \psi(x)|_{x=\pm a-0} = q_0 \psi(\pm a). \tag{A1}$$

In certain narrow regions in the bias-$k_F a$ plane, cAR is enhanced. But the enhanced cAR contributions to the conductance are much smaller even in the theoretical calculations for a ballistic system ($0.15 \times 2e^2/h$ being the largest value obtained in this setup to the maximum possible value of $2e^2/h$). The mechanism here is multiple back-and-forth reflections of the BdG quasiparticles in the SC due to the presence of barriers at the NS junctions. Though the spectrum is gapped, the evanescent BdG modes have some real component to their "momenta" and that is what amounts to saying *'multiple back-and-forth reflections.'*

Experiments so far have found a very small enhancement factor for cAR. Russo *et al.* [20] have performed experiments on a setup that is qualitatively an NM-SC-NM junction with barriers. But, this differs from the calculations here mainly in the fact that the NM's in experiments are diffusive while the calculations have been performed for NM-SC-NM keeping in mind ballistic NM's. Thus, the results of the calculations cannot be directly used to understand experiments. Nevertheless, evidence of the enhancement of cAR is found in experiments and the negative nonlocal voltage measured is of the order of 10^{-2} times the value of the normal state voltage. This

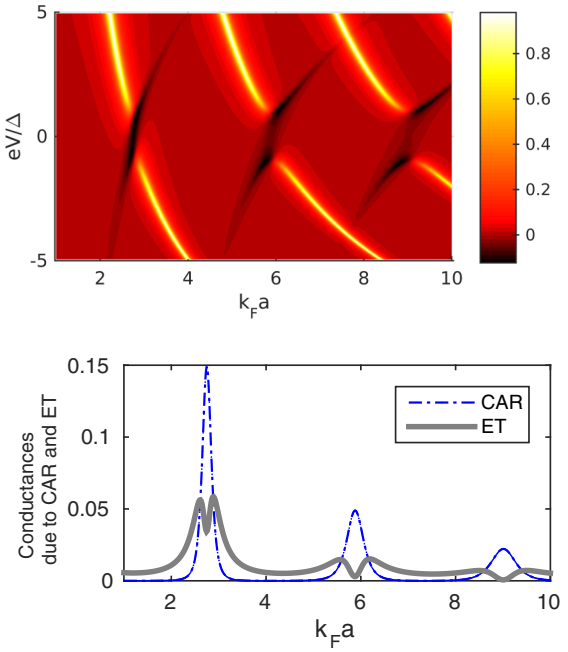

FIG. 3. Our calculation of ET and cAR contributions in a single channel NSN geometry with delta-function barriers of $q_0 = 5k_F$ at the NS junctions. G_{RL} is plotted in the upper panel as a contour plot in units of $2e^2/h$. In the lower panel, ET and cAR contributions to G_{RL} are plotted at a fixed bias $eV = 0\Delta$ as a function of the length of the SC region in units of k_F^{-1}. cAR enhancement is π periodic in $k_F a$.

is to be contrasted with the value of 0.8 that we get in our calculations. The BdG modes also have an imaginary part to the momentum in addition to the real part which suppresses the nonlocal subgap transport when the length of the SC is very large. In the opposite limit of a short SC region, the electron to hole conversion is very small. Also, in the limit of the barrier strength q_0 much smaller than the Fermi wave number k_F, the effect of the barrier becomes negligible and the dominance of ET is restored. Ideally, to enhance cAR in this setup, $k_F a \sim \pi$ and $q_0 \gtrsim k_F$ to enable a few back-and-forth reflections of the BdG quasiparticle modes before they decay (the real part of k is responsible for this interference) and electron to hole conversion to happen.

APPENDIX B: JOSEPHSON JUNCTION BETWEEN TWO-DIMENSIONAL SUPERCONDUCTORS

A system closely related to the ladder proposed here is a Josephson junction between a pair of two-dimensional superconductors. The Hamiltonian that describes such a Josephson junction is:

$$H = \sum_s \Bigg[\Psi_s^\dagger(x,y) \Bigg\{ -\left(\frac{\hbar^2}{2m}\frac{\partial^2}{\partial x^2} + \frac{\hbar^2}{2m}\frac{\partial^2}{\partial y^2} + \mu \right)\tau_z + \Delta[\cos[\phi(y)]\tau_x + \sin[\phi(y)]\tau_y] \Bigg\} \Psi_s(x,y) \Bigg],$$
$$\text{where} \quad \phi(y) = 0 \quad \text{for } y > 0,$$
$$\text{and} \quad \phi(y) = -\phi \quad \text{for } y < 0. \tag{B1}$$

The dispersion for the bulk as given by this Hamiltonian is

$$E(\vec{k}) = \pm\sqrt{(\hbar^2\vec{k}^2/2m - \mu)^2 + \Delta^2}, \tag{B2}$$

and the bulk gap is 2Δ. We show here that a nonzero ϕ can induce one-dimensional states localized at the junction. The BC for the junction is $\psi(x, y = 0^+) = \psi(x, y = 0^-)$ and $[\partial_y\psi(x,y)|_{y=0^+} - \partial_y\psi(x,y)|_{y=0^-}] = q_0\psi(x, y = 0)$. The parameter q_0 characterizes the transparency of the junction. The limits $q_0 = 0$ and $q_0 \to \infty$ correspond to fully transparent and fully opaque junctions, respectively. The subgap states require at least one out of k_x and k_y to be complex. Since the junction is in the y direction, k_y is complex. Translational invariance of the system along the x direction makes k_x a good quantum number and real valued. At a given energy E in the gap (i.e., $|E| < \Delta$) and in a particular spin eigensector s, the wave function

$$\psi(x,y) = e^{ik_x x} \cdot \sum_{\nu=\pm} A_{s_y,\nu} e^{i\nu k_R y - s_y\kappa y}\vec{u}_{s_y,\nu}, \tag{B3}$$

where $k_y = \nu k_R + i s_y\kappa$, $(k_R,\kappa > 0)$, $\vec{k} = (k_x,k_y)$, $\vec{k}$ is related to E by the dispersion relation Eq. (B2), $s_y = sign(y)$, and $\vec{u}_{s_y,\nu}$ is the eigenspinor that is a function of $k_y = \nu k_R + i s_y\kappa$. Substitution of the above wave function in the BC equation yields a subgap state that exists if and only if $\mathrm{Det}[M] = 0$, where M is 4×4 matrix, given by:

$$M = [M_1 \quad M_2], \quad \text{where}$$
$$M_1 = \begin{bmatrix} \vec{u}_{+,+} & \vec{u}_{+,-} \\ (ik_{+,+} - q_0)\vec{u}_{+,+} & (ik_{+,-} - q_0)\vec{u}_{+,-} \end{bmatrix}$$
$$M_2 = \begin{bmatrix} \vec{u}_{-,+} & \vec{u}_{-,-} \\ -ik_{-,+}\vec{u}_{-,+} & -ik_{-,-}\vec{u}_{-,-} \end{bmatrix}. \tag{B4}$$

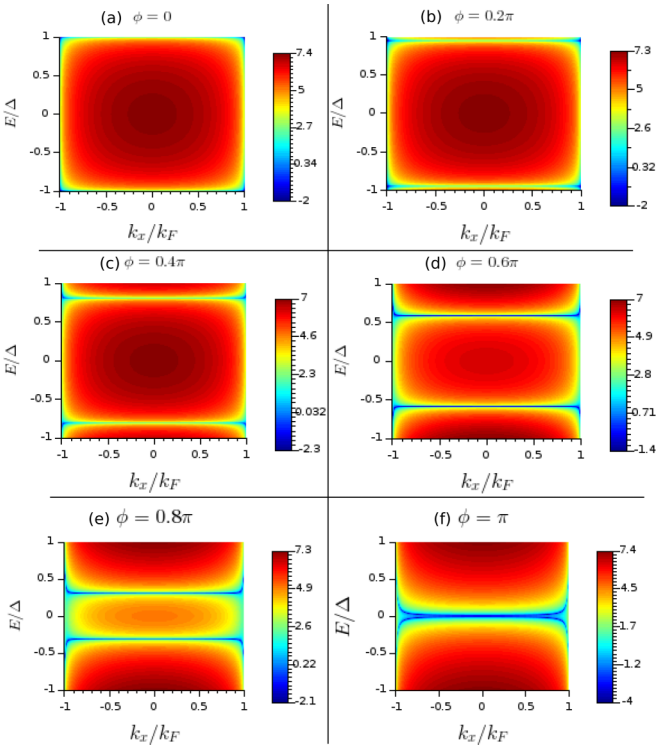

FIG. 4. $\log|\mathrm{Det}.[M]|$ plotted as a function of E and k_x for various choices of ϕ. Dark blue regions in each contour plot indicate the existence of subgap states localized along the junction. We have chosen $q_0 = 0$ everywhere.

The results of a numerical calculation presented in Fig. 4 show that a nonzero phase difference ϕ results in subgap states, that go deeper into the gap as ϕ approaches π. The dispersion of the 1D modes is almost flat in the middle, while for k_x near $\pm k_F$, the dispersion has a sharp slope and connects to energies $\pm\Delta$ smoothly.

[1] A. F. Andreev, Sov. Phys. JETP **19**, 1228 (1964).
[2] G. E. Blonder, M. Tinkham, and T. M. Klapwijk, Phys. Rev. B **25**, 4515 (1982).
[3] A. Kastalsky, A. W. Kleinsasser, L. H. Greene, R. Bhat, F. P. Milliken, and J. P. Harbison, Phys. Rev. Lett. **67**, 3026 (1991).
[4] V. Mourik, K. Zuo, S. M. Frolov, S. R. Plissard, E. P. A. M. Bakkers, and L. P. Kouwenhoven, Science **336**, 1003 (2012); S. M. Albrecht, A. P. Higginbotham, M. Madsen, F. Kuemmeth, T. S. Jespersen, J. Nygard, P. Krogstrup, and C. M. Marcus, Nature (London) **531**, 206 (2016).
[5] A. Soori and D. Sen, Europhys. Lett. **93**, 57007 (2010); Phys. Rev. B **84**, 035422 (2011); I. Safi and H. J. Schulz, *ibid.* **52**, R17040(R) (1995).
[6] C. Chamon, M. Oshikawa, and I. Affleck, Phys. Rev. Lett. **91**, 206403 (2003); M. Oshikawa, C. Chamon, and I. Affleck, J. Stat. Mech. (2006) P02008.
[7] T. Domanski, Phys. Rev. A **84**, 023634 (2011); I. Zapata and F. Sols, Phys. Rev. Lett. **102**, 180405 (2009); A. J. Daley, P. Zoller, and B. Trauzettel, *ibid.* **100**, 110404 (2008).
[8] J. M. Byers and M. E. Flatté, Phys. Rev. Lett. **74**, 306 (1995).
[9] R. Mélin, F. S. Bergeret, and A. Levy Yeyati, Phys. Rev. B **79**, 104518 (2009).
[10] G. Deutscher and D. Feinberg, Appl. Phys. Lett. **76**, 487 (2000); G. Falci, D. Feinberg, and F. W. J. Hekking, Europhys. Lett. **54**, 255 (2001).
[11] R. W. Reinthaler, P. Recher, and E. M. Hankiewicz, Phys. Rev. Lett. **110**, 226802 (2013).
[12] Wei Chen, D. N. Shi, and D. Y. Xing, Sci. Rep. **5**, 7607 (2015).
[13] S. Gomez, P. Burset, W. J. Herrera, and A. L. Yeyati, Phys. Rev. B **85**, 115411 (2012); J. Linder and T. Yokoyama, *ibid.* **89**, 020504(R) (2014); J. Linder, M. Zareyan, and A. Sudbo, *ibid.* **80**, 014513 (2009); J. Wang, L. Hao, and K. S. Chan, *ibid.* **91**, 085415 (2015); F. Crépin, H. Hettmansperger, P. Recher, and B. Trauzettel, *ibid.* **87**, 195440 (2013).
[14] J. J. He, J. Wu, T.-P. Choy, X.-J. Liu, Y. Tanaka, and K. T. Law, Nat. Commun. **5**, 3232 (2014).
[15] A. Levy Yeyati, F. S. Bergeret, A. Martin-Rodero, and T. M. Klapwijk, Nat. Phys. **3**, 455 (2007).

[16] N. M. Chtchelkatchev, JETP Lett. **78**, 230 (2003).
[17] R. Mélin and D. Feinberg, Phys. Rev. B **70**, 174509 (2004); M. Božović and Z. Radović, *ibid.* **66**, 134524 (2002); Z. C. Dong, R. Shen, Z. M. Zheng, D. Y. Xing, and Z. D. Wang, *ibid.* **67**, 134515 (2003).
[18] T. Yamashita, S. Takahashi, and S. Maekawa, Phys. Rev. B **68**, 174504 (2003).
[19] D. Beckmann, H. B. Weber, and H. v. Löhneysen, Phys. Rev. Lett. **93**, 197003 (2004); D. Beckmann and H. v. Löhneysen, AIP Conf. Proc. **850**, 875 (2006).
[20] S. Russo, M. Kroug, T. M. Klapwijk, and A. F. Morpurgo, Phys. Rev. Lett. **95**, 027002 (2005).
[21] K. Sun, N. Shah, and S. Vishveshwara, Phys. Rev. B **87**, 054509 (2013).
[22] P. Recher, E. V. Sukhorukov, and D. Loss, Phys Rev B **63**, 165314 (2001); C. Bena, S. Vishveshwara, L. Balents, and M. P. A. Fisher, Phys. Rev. Lett. **89**, 037901 (2002).
[23] A. Das, Y. Ronen, M. Heiblum, D. Mahalu, and A. V. Kretinin, Nat. Commun. **3**, 1165 (2012).
[24] J. Schindele, A. Baumgartner, and C. Schönenberger, Phys. Rev. Lett. **109**, 157002 (2012).
[25] D. Gosselin, G. Hornecker, R. Mélin, and D. Feinberg, Phys. Rev. B **89**, 075415 (2014).
[26] M. Carreau, E. Farhi, and S. Gutmann, Phys. Rev. D **42**, 1194 (1990).
[27] R. Landauer, IBM J. Res. Dev. **1**, 223 (1957); Philos. Mag. **21**, 863 (1970); M. Büttiker, Y. Imry, R. Landauer, and S. Pinhas, Phys. Rev. B **31**, 6207 (1985); M. Büttiker, Phys. Rev. Lett. **57**, 1761 (1986); S. Datta, *Electronic Transport in Mesoscopic Systems* (Cambridge University Press, Cambridge, 1995).
[28] Though exact expression for k_i needs to be obtained by inverting the dispersion Eq. (2) as explained in the text after Eq. (3), the approximation $k_i = \sqrt{2m\mu_i/\hbar^2}$ is valid when $\mu \gg g > \Delta \geqslant |E|$.
[29] A. Soori, S. Das, and S. Rao, Phys. Rev. B **86**, 125312 (2012).
[30] M. Tinkham, *Introduction to Superconductivity* (McGraw-Hill, New York, 1975), Chap. 6.
[31] A. Keselman, L. Fu, A. Stern, and E. Berg, Phys. Rev. Lett. **111**, 116402 (2013).
[32] D. Z. Liu, K. Levin, and J. Maly, Phys. Rev. B **51**, 8680(R) (1995).
[33] J.-D. Pillet, C. H. L. Quay, P. Morfin, C. Bena, A. Levy Yeyati and P. Joyez, Nat. Phys. **6**, 965 (2010).